멤브레인(Membrane Journal)
Vol. 34 No. 3 June 2024, 192-203

Print ISSN: 1226-0088
Online ISSN: 2288-7253
DOI: https://doi.org/10.14579/MEMBRANE_JOURNAL.2024.34.3.192

고분자량 PEO 기반 분리막에 대한 다양한 고분자 첨가제의 영향 분석

민 효 준[1] · 손 영 재[1] · 김 종 학[†]

연세대학교 화공생명공학과

(2024년 5월 1일 접수, 2024년 6월 7일 수정, 2024년 6월 7일 채택)

Polymeric Additive Influence on the Structure and Gas Separation Performance of High-Molecular-Weight PEO Blend Membranes

Hyo Jun Min[1], Young Jae Son[1], and Jong Hak Kim[†]

Department of Chemical and Biomolecular Engineering, Yonsei University, Seoul 03722, Korea

(Received May 1, 2024, Revised June 7, 2024, Accepted June 7, 2024)

요 약: 기체 분리막의 상업적 발전은 CO_2 분리 효율을 향상시키는 데 중요한 역할을 한다. 고분자량 PEO (high-Mw PEO)는 높은 CO_2 용해도, 가격 경쟁성 및 견고한 기계적 특성을 가져 분리막 제조용 고분자로 유력하지만 그 특유의 결정성으로 인해 기체 분리막에 응용이 어렵다. 본 연구에서는 결정성 감소를 위해 다양한 고분자 첨가제를 고분자량 PEO에 혼합하는 방법을 제시하였다. 폴리에틸렌글리콜(PEG), 폴리프로필렌글리콜(PPG), 폴리아크릴산(PAA) 및 폴리비닐피롤리돈(PVP)과 같은 상업적으로 이용 가능하고 섞임성이 좋은 수용성 고분자를 첨가제로 사용하여 PEO 결정성을 감소시킴으로써 가스 분리 성능을 향상시키고자 하였다. PEG 및 PPG의 경우 PEO의 결정 구조를 억제하지 못하고 분리막의 결함을 초래하였으나, PAA 및 PVP는 PEO의 결정 구조를 바꿔 결함이 없는 분리막을 제조하는 데 성공하였다. 고분자량 PEO 혼합막의 결정 구조 변화와 기체 분리 성능의 상관관계를 조사하여 본 연구의 결과와 이전에 기록된 결과를 바탕으로 고분자량 PEO에 대한 첨가제 고분자의 설계 및 선택에 대한 통찰력을 제공하며, 이를 통해 비용 효율적이고 상업적으로 실용적인 CO_2 분리막을 제조하고자 하였다.

Abstract: The advancement of commercially viable gas separation membranes plays a pivotal role in improving CO_2 separation efficiency. High-molecular-weight poly(ethylene oxide) (high-Mw PEO) emerges as a promising option due to its high CO_2 solubility, affordability, and robust mechanical attributes. However, the crystalline nature of high-Mw PEO hinders its application in gas separation membranes. This study proposes a straightforward blending approach by incorporating various polymeric additives into high-Mw PEO to address this challenge. Four commercially available, water-soluble polymers, i.e. poly(ethylene glycol) (PEG), poly(propylene glycol) (PPG), poly(acrylic acid) (PAA), and poly(vinyl pyrrolidone) (PVP) are examined as additives to enhance membrane performance by improving miscibility and reducing PEO crystallinity. Contrary to expectations, PEG and PPG fail to inhibit the crystalline structure of PEO and result in membrane flaws. Conversely, PAA and PVP demonstrate greater success in altering the crystal structure of PEO, yielding defect-free membranes. A thorough investigation delves into the correlation between changes in the crystalline structure of high-Mw PEO blend membranes and their gas separation performance. Drawing from our findings and previously documented outcomes, we offer insights into designing and selecting additive polymers for high-Mw PEO, aiming at the creation of cost-effective, commercially viable CO_2 separation membranes.

Keywords: *poly(ethylene oxide), polymer blend, CO_2, gas separation, membrane*

[1] The authors equally contributed to this work.

[†]Corresponding author(e-mail: jonghak@yonsei.ac.kr; http://orcid.org/0000-0002-5858-1747)

1. Introduction

Elevated atmospheric levels of carbon dioxide (CO_2), primarily attributed to human activities like industrial processes and the burning of fossil fuels, have sparked urgent concerns regarding global warming and climate change[1,2]. Addressing these challenges requires innovative solutions to mitigate CO_2 emissions and steer toward a more sustainable trajectory. A promising avenue for CO_2 capture is through membrane separation processes, offering advantages such as energy efficiency, scalability, and reduced environmental impact compared to conventional methods such as absorption or cryogenic distillation[3,4].

Poly(ethylene oxide) (PEO) has emerged as a notable contender among various membrane materials for CO_2 separation, garnering attention for its favorable properties[5,6]. PEO-based membranes demonstrate high selectivity for CO_2 due to the quadrupole-dipole interaction between CO_2 molecules and ether groups within the polymer structure[7]. Various strategies have been investigated to utilize PEO in gas separation membranes. These include synthesizing PEO-based copolymers, blending PEO with other polymers, creating mixed-matrix membranes (MMMs) with fillers, and preparing crosslinked poly(ethylene glycol diacrylate) (XLPEGDA)[8-13]. Commercial block copolymers such as Pebax and Polyactive, derived from PEO, have been developed to advance gas separation membrane technology[8,14]. Among these approaches, polymer blending stands out as one of the most effective methods for preparing gas separation membranes, owing to its cost-effectiveness, simplicity, and scalability[5].

High-molecular-weight PEO (high-Mw PEO) emerges as a highly promising material for CO_2 separation membranes, offering robust mechanical strength and affordability, rendering it suitable for industrial applications[15]. The good solubility in mild solvents such as water and ethanol, and cost-effectiveness of high-Mw PEO membranes position them as an appealing choice for industries seeking sustainable and economical CO_2 capture solutions. However, despite its potential, the crystalline structure of high-Mw PEO presents challenges for membrane usage[6,16]. The presence of densely packed polymer chains within crystalline domains impedes gas transport properties, resulting in inadequate membrane permeability[17]. Additionally, defects arising from the growth of PEO crystals limit the overall performance of high-Mw PEO membranes[18]. Overcoming these limitations necessitates enhancing the amorphous regions within the PEO matrix while minimizing defects.

To address these challenges, we introduced four distinct types of amorphous and polar polymer—poly(ethylene glycol) (PEG), poly(propylene glycol) (PPG), poly(acrylic acid) (PAA), and poly(vinyl pyrrolidone) (PVP)—to investigate the effect polymer additives on the high-Mw PEO-based blend membranes. These polymers feature functional groups capable of interacting strongly with PEO through hydrogen bonding or dipole-dipole interactions. By modulating the interactions between polymer chains, we aimed to restrain PEO chain packing and suppress the formation of defects between PEO spherulites, thereby facilitating the diffusion of gas molecules through the membrane with enhanced selectivity. We systematically investigated the effects of these polymers on the crystalline structures and gas separation performances of the PEO-based membranes using a straightforward blending approach. The crystallinity of PEO in the membranes was assessed through various analyses, including X-ray diffraction (XRD), differential scanning calorimetry (DSC), and small-angle X-ray scattering (SAXS). Gas separation performances were evaluated under conditions of 1 atm and 35°C. By correlating the crystalline structure of the PEO-blend membranes with their gas separation performances, we propose guidelines for selecting additive polymers in high-Mw PEO to prepare gas separation membranes using simple, cost-effective methods.

2. Experimental

2.1. Materials

Poly(ethylene oxide) (PEO, average molecular weight:

1,000,000 g mol^{-1}), poly(ethylene glycol) (PEG, Mv ~400 g mol^{-1}), poly(propylene glycol) (PPG, Mv ~425 g mol^{-1}), poly(acrylic acid) (PAA, Mw ~1,800 g mol^{-1}) and poly(vinyl pyrrolidone) (PVP, Mw ~40,000 g mol^{-1}) was purchased from Sigma-Aldrich. Deionized water and ethanol (99% purity) were obtained from Duksan Reagent & Chemicals. All the materials were used without further purification.

2.2. Preparation of PEO blend membranes

High-Mw PEO was dissolved in a solvent comprising 95% ethanol and 5% water at a concentration of 2 w/v%, followed by vigorous stirring at 50°C for 24 hours. An appropriate amount of the selected polymer additive (PEG, PPG, PAA, or PVP) was introduced into the solution to achieve a 30 wt% blend membrane. The mixture underwent overnight stirring to ensure uniformity. Subsequently, the solution was poured into a Teflon dish covered with aluminum foil punctured with pinholes to regulate evaporation rate. The dish was then placed in a drying oven at 50°C for two days and completely dried in a vacuum oven. The resulting membranes were denoted as PEO/PEG, PEO/PPG, PEO/PAA, and PEO/PVP based on the incorporated polymers.

2.3. Gas separation measurements

The gas permeabilities and diffusivity of the dense polymeric membranes were evaluated at a temperature of 35°C using a time lag technique with a constant volume/variable pressure apparatus provided by Airrane Co., Ltd., Korea. The membranes had an active area of 15.2 cm^2. Gas permeability was determined using the time-lag method, which involved monitoring the increase in downstream pressure within a fixed volume at an upstream pressure of 760 torr. The results for gas permeability were reported in units of barrer, where 1 barrer equals 1×10^{-10} cm^3 (STP) $cm/cm^2 \times s \times cmHg$. CO_2/N_2 selectivity was calculated by dividing the permeability values for each pure gas.

2.4. Characterizations

The interactions between high-Mw PEO and the polymer additives were examined using an FT-IR spectrometer (Spectrum Two, Perkin Elmer, USA). X-ray diffraction (XRD) analysis (D8 Advance, Bruker, Germany) was conducted with a scanning speed of 2° min^{-1} across the 2θ range of 5~50° to investigate the crystalline structure of PEO in the PEO blend membranes. Thermal properties and the degree of crystallinity of PEO within the membranes were analyzed via differential scanning calorimetry (DSC; Discovery DSC, TA Instrument) at a heating rate of 20°C min^{-1} under a N_2 atmosphere. Small-angle X-ray scattering (SAXS) patterns were obtained for characterizing the lamellar crystallites of PEO using the 4C SAXS beamline at the Pohang Light Source, Korea.

3. Result and Discussion

3.1. Preparation of PEO blend membranes

Four distinct polymers—PEG, PPG, PVP, and PAA—were selected as additives to modulate the crystalline structure of PEO due to their shared hydrophilicity and compatibility with benign solvents such as water or alcohol, owing to the presence of strong polar groups such as ether, carbonyl, or hydroxyl groups. These groups are anticipated to interact strongly with the ether groups of PEO, promoting excellent miscibility. Moreover, being amorphous at room temperature, these polymers are expected to diminish the crystallinity of PEO. The flexible chain structures of these polymers facilitate intermolecular entanglement, disrupting the regular packing of crystalline chains and impeding the formation of crystalline domains. Consequently, the overall degree of crystallinity in the blend membrane is reduced, akin to a plasticizer effect. This results in a more disordered chain arrangement and lower crystallinity compared to pure crystalline polymer, thereby increasing the free volume and gas diffusivity of the membranes.

PEO and PEG share similar repeating units of ethylene oxide, with PEG typically referring to lower molecular weight polymers. Despite the propensity for crystallization based on ethylene oxide groups, PEG

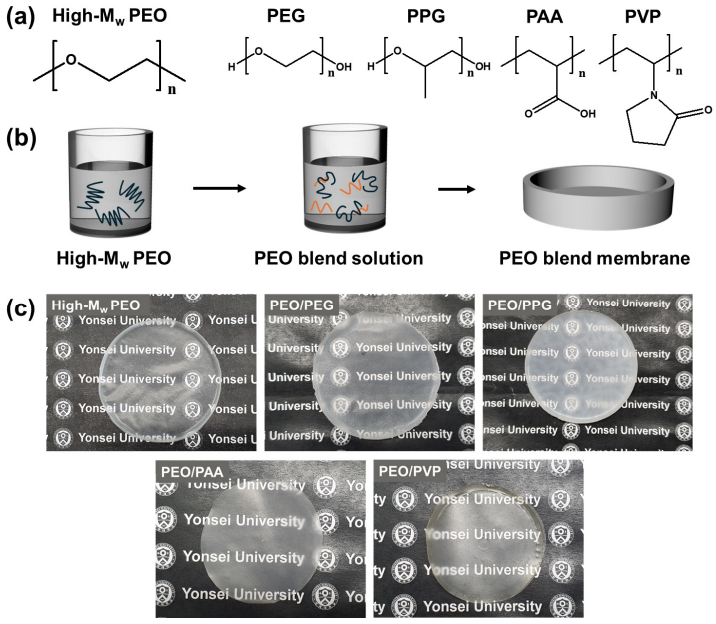

Fig. 1. (a) Chemical structure of high-Mw PEO, PEG, PPG, PAA, and PVP, (b) schematic illustration of the process to fabricate PEO blend membranes, (c) photo of high-Mw PEO and PEO blend membranes.

with a molecular weight below 1,000 g mol^{-1} is known to exist in an amorphous state. While it exhibits high CO_2 permeability and selectivity, its liquid state at room temperature poses challenges for its application in gas separation membranes. Consequently, considerable research has focused on using it as an additive polymer in polymeric membranes to enhance its performance[19,20]. However, despite its high potential, PEO/PEG blend membranes have not been extensively analyzed. Due to their chemical structural similarity, PEG and PEO are expected to exhibit good miscibility, with PEO compensating for the poor mechanical properties of PEG, rendering them suitable for gas separation membrane applications.

PPG shares very similar chemical structures with PEO but possesses more hydrophobic properties due to the additional methyl group in its repeating units. The presence of the methylene group disrupts the dense chain packing of PEO, thereby reducing its crystallinity upon the addition of PPG[21,22]. Block copolymers composed of PEG and PPG blocks are commonly used in gas separation applications for this reason[23,24]. We anticipate PPG playing a similar role in high-Mw PEO membranes. PAA can form robust hydrogen bonding interactions with PEO owing to the presence of the carboxylic acid group[25]. This interaction involves the donation of a hydrogen bond from the carboxyl group of PAA to the ether linkages or hydroxyl groups of PEO[26], facilitating the formation of hydrogen-bonded networks that enhance miscibility and intermolecular interactions between the polymers. PVP is another additive polymer utilized in polymer blend composites, known for its high polarity and miscibility [27]. It exhibits strong compatibility with PEO based on robust dipole-dipole interactions. The carbonyl oxygen atom in PVP carries a partial negative charge, while the carbon atom bears a partial positive charge. This polarity enables strong dipole-dipole interactions between the oxygen atoms of PEO and the carbonyl groups of PVP, promoting the miscibility and compatibility of the polymer blend[28]. PVP aids in mitigating defects and enhancing the overall gas permeability of the membrane while preserving selectivity.

We conducted an investigation into the impact of these polymers on PEO, particularly focusing on the crystalline structure of PEO, which is crucial for the

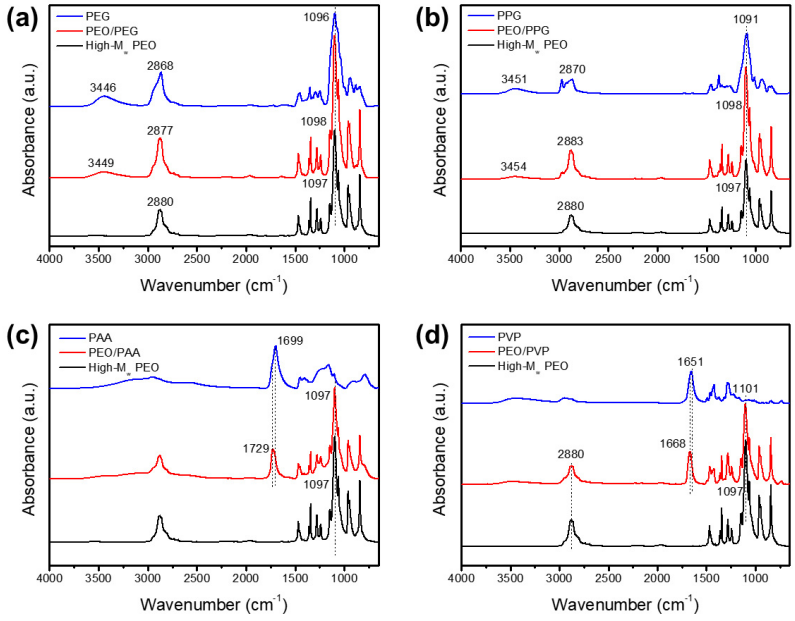

Fig. 2. FT-IR spectra of high-M_w PEO and polymer additive; (a) PEG, (b) PPG, (c) PAA, and (d) PVP and their blend membranes.

application of gas separation membranes. We anticipated the intrusion of amorphous polymer chains into crystalline PEO domains, thereby characterizing their effect on the crystalline structure. The membranes were prepared using simple blending and solution-casting techniques. PEO was dissolved in an ethanol/water mixture, and the additive polymer was introduced into the solution. The solution exhibited a slightly opaque appearance due to the presence of crystalline PEO. Subsequently, the solution was cast onto a Teflon dish to fabricate free-standing membranes, as depicted in Fig. 1b. The high-Mw PEO membrane appeared translucent due to its semi-crystalline nature. Additionally, the surface of the high-Mw PEO membrane displayed roughness and unevenness, attributed to the formation of crystalline spherulites. In the case of PEO/PEG and PEO/PPG membranes, the surface roughness remained unchanged, and the color of the PEO/PPG membrane even intensified. However, PEO/PVP and PEO/PAA membranes exhibited smoother surfaces, potentially indicating a reduction or elimination of spherulite sizes. Moreover, these membranes appeared clearer and more transparent compared to others.

3.2. Characterization of PEO blend membranes

The interaction between the polymers was assessed using FT-IR analysis, as shown in Fig. 2. We examined the band shifts of both PEO and additive polymers post-blending. In the case of high-Mw PEO, particular attention was given to two prominent bands at around 2880 and 1097 cm^{-1}, corresponding to methylene stretching and ether bond group stretching, respectively. The stretching vibration peak of C–O–C manifested as three peaks at 1060, 1097, and 1145 cm^{-1}, indicative of the strong crystallinity of PEO[29]. PEG, lacking the triplet observed in high-Mw PEO spectra, indicated an amorphous state due to its lower molecular weight. The -OH group bands of PEG around 3446 cm^{-1} exhibited a slight shift to 3449 cm^{-1}, suggesting weak interaction with the PEO membrane. However, discerning changes in the ether bond of PEG proved challenging due to overlap with that of PEO. Similar observations were made following the addition of PPG, with only minor shifts observed in methylene and hydroxyl group stretching. Despite the potential for strong hydrogen bonding between the hydroxyl groups of PEG and PPG with PEO, their limited presence im-

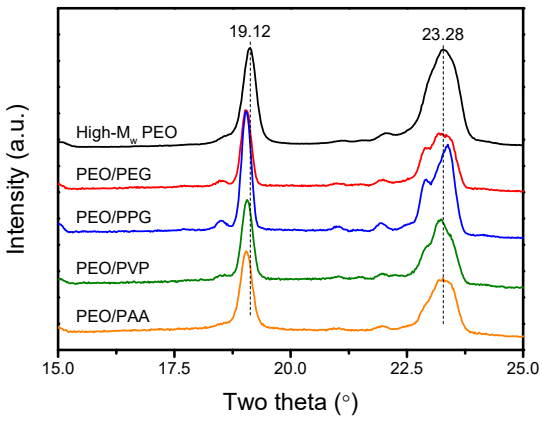

Fig. 3. XRD patterns of high-M_w PEO and the PEO blend membranes with different additive polymers.

pedes significant interchain interactions. In contrast, a substantial shift in the carboxyl group bands of PAA from 1699 cm^{-1} to 1729 cm^{-1} was observed in the PEO/PAA membrane, indicating strong interaction between PAA and PEO via hydrogen bonding. This interchain interaction between PAA and PEO, driven by hydrogen bonding, resulted in a blue shift of the carboxyl group. Intriguingly, no observable band shift was noted for the ether bond of PEO. Similarly, in the PEO/PVP membrane, a notable shift in the carbonyl group bands of PVP from 1651 cm^{-1} to 1668 cm^{-1} indicated strong interaction with PEO. Additionally, the ether bond of PEO shifted from 1097 cm^{-1} to 1101 cm^{-1}, suggesting alterations in the chain packing of high-Mw PEO. The FT-IR analysis revealed that polymers with polar groups interacted with the ether bonds of PEO, influencing the crystalline structure of the membrane.

The crystalline structures of the membranes were further analyzed using XRD and DSC techniques. Firstly, XRD patterns of the membranes were examined, as shown in Fig. 3. The two prominent peaks of high-Mw PEO observed around 19.1° and 23.3° correspond to the (120) and (112) planes, respectively[30]. Interestingly, PEO/PEG and PEO/PPG membranes also exhibited strong peaks despite the reduction in the overall PEO content in the membrane. This suggests that the crystallinity of PEO within the membrane was not significantly affected by the incorporation of PEG or PPG. Conversely, PEO/PAA and PEO/PVP membranes displayed much lower intensity peaks, indicating a decrease in the crystallinity of PEO.

The degree of crystallinity of PEO in the membrane was quantified using DSC data. Initially, the melting temperature (T_m) of PEO crystals was observed at 64.0°C for the pristine high-Mw PEO membrane. Upon the addition of amorphous polymers, the Tm decreased due to polymer-polymer interactions[31]. The crystallinity of PEO was determined by measuring the heat of fusion during PEO melting.

$$X_{c,total}(\%) = \frac{\triangle H_m}{\triangle H^o_{m,PEO}} \times 100 \quad (1)$$

$$X_{c,PEO}(\%) = \frac{\triangle H_m \times w_{PEO}}{\triangle H^o_{m,PEO}} \times 100 \quad (2)$$

where $\triangle H_m$ is the calculated fusion enthalpy per gram of the membrane which is measured from the melting peak in DSC. $\triangle H^o_{m,PEO}$ is the heat of melting per gram of 100% crystalline PEO with the molecular weight of 10^6 g mol^{-1}, reported as 205 J g^{-1}[32]. w_{PEO} is the weight fraction of PEO in the PEO blend membrane, which is 0.3 in this study. In the PEO/PEG blend, the degree of crystallinity of PEO experienced a slight increase from 66.4% to 66.9%. This suggests that PEG might have struggled to penetrate through the densely packed PEO chains. Conversely, in the case of PEO/PPG, the degree of crystallinity of PEO exhibited a more notable increase, rising to 69.4%. The hydrophobic methylene group of PPG likely induced denser chain packing of PEO, consistent with both XRD results and the observed opaque, bumpy surfaces of the membranes. Despite expectations, the high crystallinity of high-Mw PEO, combined with the influence of the $-CH_3$ group in PPG, contributed to an increase in crystallinity rather than disrupting chain packing.

While both PEG and PPG are commonly employed as plasticizers in other polymers due to their amor-

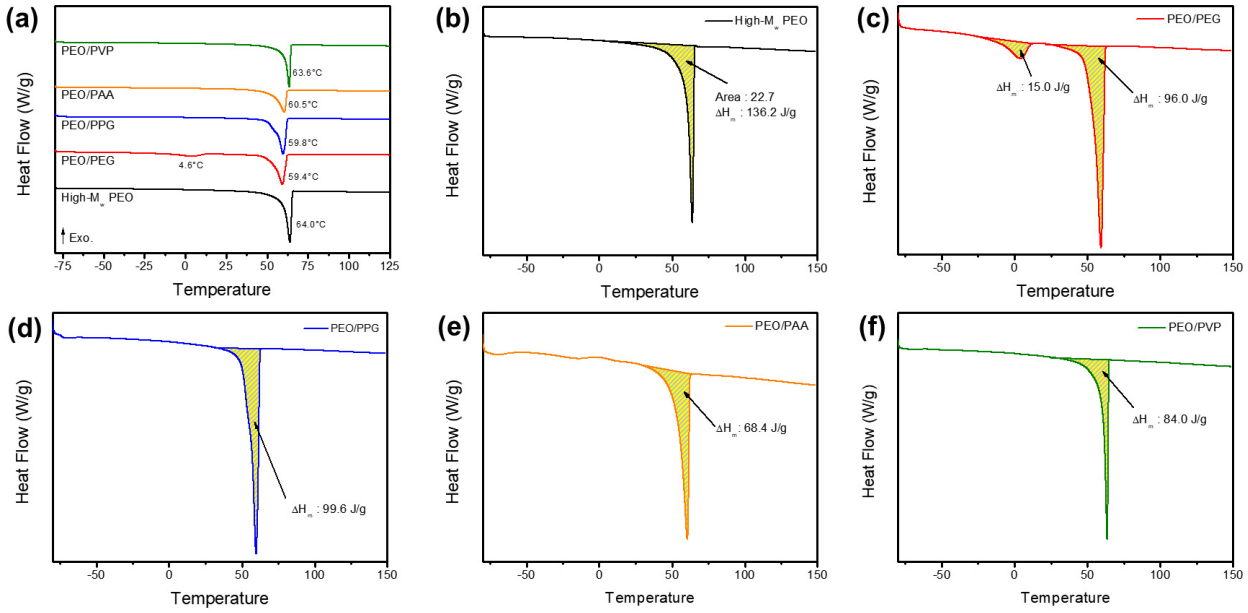

Fig. 4. (a) DSC curves of high-M_w PEO and PEO/blend membranes and (b-f) their magnified curves with the calculated heat of enthalpy per gram of membrane.

Table 1. Melting Temperature ($T_{m,\ PEO}$), Heat of Fusion ($\triangle H_{m,\ PEO}$), Glass Transition Temperature[12], and Degree of Crystallinity (X_c) of Blend Membranes Obtained from DSC

Sample	$T_{m,\ PEO}$ (°C)	$\triangle H_{m,\ PEO}$ (J g^{-1})	T_g (°C)	$X_{c,\ PEO}$ (%)	$X_{c,\ total}$ (%)
High-M_w PEO	64.0	136.2	-60.2	66.4	66.4
PEO/PEG	59.4	96.0	-60.5	66.9	46.8
PEO/PPG	59.8	99.6	-71.0	69.4	48.6
PEO/PAA	60.5	68.4	-67.0	47.7	33.4
PEO/PVP	63.6	84.0	-59.9	58.6	41.0

phous nature, they proved ineffective in reducing crystallinity within the PEO matrix. Conversely, a significant decrease in crystallinity was observed in PEO/PAA and PEO/PVP blends. In these cases, the crystallinity of PEO dropped to 47.7% and 58.6% for PEO/PAA and PEO/PVP, respectively. The strong interaction between PAA and PEO led to a sharp decrease in PEO crystallinity. However, it is important to note that the degree of crystallinity alone does not fully describe the overall crystalline structure of the membranes. Further detailed characterization is necessary to investigate the microstructure of PEO crystals within the membranes.

For semi-crystalline polymers such as PEO, the formation of lamellar crystals progresses into crystalline fibrils or spherulites. High-Mw PEO is known to develop crystalline spherulites originating from lamellar crystals[33]. Interspherulitic defects, occurring between the spherulites, are often the primary cause of defects in PEO membranes used for gas separation. Therefore, it is crucial to prevent the formation of these defects to enable the application of high-Mw PEO in gas separation membranes. While thermal treatment near the melting temperature of PEO can reduce these defects, it necessitates additional processes and costs and may potentially harm the membranes. In crystalline/amorphous polymer blends, the segregation of the amorphous phase influences crystallization[34]. Hence, it's essential

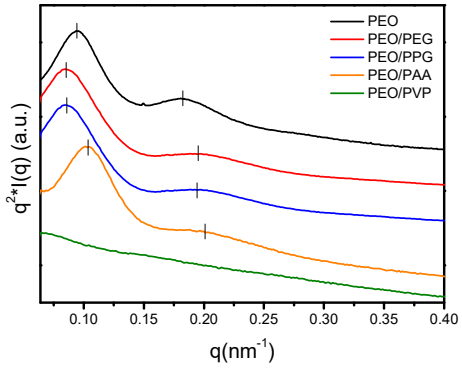

Fig. 5. SAXS spectra of high-Mw PEO and PEO blend membranes with different additive polymers.

to characterize which type of phase morphologies (such as interlamellar, interfibrillar, interspherulitic segregation, and intralamellar) of the additive amorphous polymer predominates in the blend membranes[35,36].

SAXS analysis serves as a potent tool for investigating the lamellar microstructure of membranes. In the SAXS graph of pristine high-Mw PEO, a distinct lamellar structure was evident, with peaks appearing at a ratio of 1:2:3, indicative of a well-defined lamellar structure comprising the continuous crystalline region and the amorphous region of PEO. Utilizing Bragg's law, the d-spacing from the peak was calculated as 66.7 nm, representing the sum of the crystalline and amorphous thicknesses of PEO. However, in the case of PEO/PEG and PEO/PPG membranes, the peak ratio deviated from the lamellar structure, appearing around 1:2.3. This deviation can be attributed to the disorder in the lamellar structure caused by the interference of the additive polymer. It is speculated that the amorphous PEG or PPG polymer randomly penetrated within the amorphous phase of PEO, as evidenced by the unchanged crystallinity of PEO upon incorporation of PEG or PPG. The substantially increased d-spacing of PEO indicates segregation of PEG or PPG within the interlamellar amorphous region of PEO crystals. This random increase in amorphous thickness led to structural irregularity in the lamellar structure of PEO crystals. The PEO/PAA membrane displayed two peaks with a ratio of 1:2, suggesting the presence of a lamellar structure. However, a peak shift was observed, indicating a decrease in lamellar thickness from 66.7 nm to 61.0 nm. This decrease is attributed to the reduced crystalline thickness of PEO crystals, corroborating the significantly decreased crystallinity observed in the DSC results. Additionally, PAA was inferred to be present not only in the interlamellar region but also in the interspherulitic region of PEO, potentially preventing the formation of interspherulitic defects in the membrane. In contrast, no strong peaks were observed in the SAXS graph of the PEO/PVP membrane, suggesting the destruction of the lamellar structure by the incorporation of PVP. Thus, PVP was found to be effective in decreasing the crystallinity of PEO and preventing the formation of lamellar crystals, potentially attributed to segregation at the intralamellar phase of PEO.

3.3. Gas separation performance of PEO blend membranes

The pure gas permeability of CO_2 and N_2 of the PEO-based membranes was measured at 1 atm and 35°C using the time-lag method. The pure PEO membrane exhibited defects due to the presence of defects

Table 2. SAXS Profiles of High-Mw PEO and PEO Blend Membranes

Sample	1st peak (nm^{-1})	2nd peak (nm^{-1})	3rd peak (nm^{-1})	Ratio	*d*-spacing (nm)
PEO	0.0942	0.181	0.274	1 : 1.92 : 2.91	66.7
PEO/PEG	0.0852	0.195	-	1 : 2.28	73.7
PEO/PPG	0.0858	0.194	-	1 : 2.26	73.2
PEO/PAA	0.103	0.201	-	1 : 1.95	61.0
PEO/PVP	-	-	-	-	-

Table 3. CO_2 Permeance and CO_2/N_2 Selectivity of PEO Blend Membranes and Previously Reported PEO-Based Blend Membranes

Membrane	PEO	Additive polymer			Gas separation performance			Reference
	Molecular weight (g mol^{-1})	Polymer	Content	Molecular weight (g mol^{-1})	CO_2 (barrer)	N_2 (barrer)	CO_2/N_2 Selectivity	
PEO	10^6	-	-	-		Defective		This work
PEO/PEG	10^6	PEG	30 wt%	400		Defective		This work
PEO/PPG	10^6	PPG	30 wt%	425		Defective		This work
PEO/PAA	10^6	PAA	30 wt%	1800	0.728	0.035	20.8	This work
PEO/PVP	10^6	PVP	30 wt%	40,000	19.9	0.98	20.3	This work
Thermally-treated PEO	10^6	-	-	-	13	0.24	55	[17]
CA/PEG	2×10^4	Cellulose acetate	40 wt%	-	7.49	0.21	36.2	[37]
PEO/PDMS-PEGBEM	10^6	PDMS-PEGBEM	50 wt%	30,000	240	6.93	34.6	[38]
PEO/PAMAM	10^6	PAMAM	10 wt%	-	32.3	0.77	42	[39]
PEO/trehalose	10^5	trehalose	15 %	342	117	2.29	51	[40]
PEO/5-hydroxy isophthalic acid	6×10^5	5-hydroxy isophthalic acid	0.5 mol%	182	573	17.7	32.4	[41]
PEO/PGP-POEM	10^6	PGP-POEM	30 wt%	-	120.9	2.69	44.9	[15]
PEO/PEGDEI	10^6	PEGDE-PEI	50 wt%	-	201.1	4.1	49.3	[18]

between the crystalline spherulites, leading to gas leakage. Similarly, both PEG and PPG-based blend membranes showed defects. Interestingly, we observed an increase in the crystallinity of PEO in the membrane upon addition of the amorphous polymer. This increase in crystallinity can be attributed to the segregation of PEG or PPG within the amorphous layer of the lamellar crystals of PEO, failing to reduce the crystallinity and prevent defect formation. One significant reason for this result is the short chain length of PEG or PPG polymers, hindering their effective entanglement among the PEO chains and crystals. Research on PEG blend membranes with varying molecular weights has shown similar findings. Additionally, increasing the molecular weight of PEG or PPG may not be effective in improving gas separation performance, as it may further increase the crystallinity of the polymer. To address this issue, previous studies have suggested the use of poly(oxyethylene methacrylate) (POEM)-based copolymers as additives for PEO-based membranes. POEM, despite its high molecular weight, maintains amorphous properties and can effectively entangle with high-Mw PEO crystals, potentially preventing crystalline defects.

In contrast, the gas separation performance of the PAA-based membrane indicated no defects between the PEO crystalline spherulites, likely due to strong hydrogen bonding between PAA and PEO. However, the gas permeability of the PEO/PAA membrane was extremely low, attributed to the inferior gas separation performance of PAA. The PEO/PVP membrane exhibited the best gas separation performance among the prepared membranes. PVP, with a molecular weight long enough to entangle with PEO chains, effectively eliminated lamellar crystals, resulting in a defect-free membrane. However, the gas separation performance was not optimal compared to reported PEO-based membranes, likely due to the inferior CO_2 separation performance of PVP.

In conclusion, while the selected commercially-available, amorphous, water-soluble polymers showed promise in enhancing gas separation performances, the re-

sults were not sufficient for practical application as gas separation membranes. Guidelines for designing additive polymers include considerations for strong interactions with PEO, sufficient molecular weight for entanglement with PEO crystals, and high gas separation performance. Other approaches such as branched polymers or crosslinking could also be explored to prevent PEO chain packing and induce segregation of additive polymers in interspherulitic defects. Further research in this area holds promise for the development of high-performance gas separation membranes based on high-Mw PEO using low-cost, simple blending methods.

4. Conclusion

In this study, we assessed commercially-available, water-soluble amorphous polymers (PEG, PPG, PAA, and PVP) as additives in high-Mw PEO to fabricate high-performance gas separation membranes. These polymers were chosen for their polar and hydrophilic properties, anticipating good compatibility with PEO in solution. Membranes were then produced using a simple blending technique. However, despite initial hopes for enhanced compatibility and interaction with PEO, both PEG and PPG failed to reduce the crystallinity of PEO. Their short chain lengths led to segregation within the amorphous regions of PEO rather than within the crystalline domain during PEO crystal growth. Consequently, the membranes exhibited defects, allowing gases to diffuse through the gaps between the crystalline spherulites. In contrast, PAA and PVP effectively disrupted the chain packing of PEO, lowering its crystallinity. Our SAXS results suggest that PAA segregated not only along the crystalline chains of PEO but also within the interspherulitic region, preventing interspherulitic defects. The lamellar crystalline structure of PEO was notably diminished in the PEO/PVP membrane, indicating the efficacy of PVP in reducing the crystallinity of high-Mw PEO. Consequently, membranes with added PAA and PVP were defect-free. However, their overall impact on gas separation performance was adverse. Given the economic and commercial feasibility of using high-Mw PEO in gas separation membrane production, a thorough design of the additive polymer is essential.

Acknowledgements

This work was supported by the National Research Foundation (NRF) of Korea, funded by the Ministry of Science and ICT (RS-2024-00333678) and the Korea Institute of Energy Technology Evaluation and Planning (KETEP) grant funded by the Korea government (MOTIE) (20214000000090, Fostering human resources training in advanced hydrogen energy industry).

Reference

1. Y. S. S. Young and R. Patel, “Ionic liquid consisted of composite membrane for carbon dioxide separation: A review”, *Membr. J.*, **33**, 240 (2023).
2. Y. Yuan, F. Shi, Q. Li, Y. Yang, X. Cai, M. Sheng, and Z. Wang, “Large-scale preparation of composite membranes for CO_2 separation via interfacial polymerization: Monomer selection and processing parameter optimization”, *J. Membr. Sci.*, **698**, 122622 (2024).
3. I. Hossain, A. Husna, and H. B. Park, “1,3-Dioxolane-based CO_2 selective polymer membranes for gas separation”, *Membr. J.*, **33**, 94 (2023).
4. S. Li, Y.-J. Sun, Z.-X. Wang, C.-G. Jin, M.-J. Yin, and Q.-F. An, “Rapid fabrication of high-permeability mixed matrix membranes at mild condition for CO_2 capture”, *Small*, **19**, 2208177 (2023).
5. S. L. Liu, L. Shao, M. L. Chua, C. H. Lau, H. Wang, and S. Quan, “Recent progress in the design of advanced PEO-containing membranes for CO_2 removal”, *Prog. Polym. Sci.*, **38**, 1089 (2013).
6. A. Kargari and S. Rezaeinia, “State-of-the-art modification of polymeric membranes by PEO and PEG for carbon dioxide separation: A review of the current status and future perspectives”, *J. Ind.*

Eng. Chem., **84**, 1 (2020).
7. W.-S. Sun, M.-J. Yin, W.-H. Zhang, S. Li, N. Wang, and Q.-F. An, "Green techniques for rapid fabrication of unprecedentedly high-performance PEO membranes for CO_2 capture", *ACS Sustain. Chem. Eng.*, **9**, 10167 (2021).
8. E. S. Yi, S. R. Hong, and H. K. Lee, "CO_2 separation performance of pebax mixed matrix membrane using PEI-GO@ZIF-8 as filler", *Membr. J.*, **33**, 23 (2023).
9. H. J. Min, M. Kang, Y.-S. Bae, R. Blom, C. A. Grande, and J. H. Kim, "Thin-film composite mixed-matrix membrane with irregular micron-sized UTSA-16 for outstanding gas separation performance", *J. Membr. Sci.*, **669**, 121295 (2023).
10. A. Ghadimi, S. Norouzbahari, V. Vatanpour, and F. Mohammadi, "An investigation on gas transport properties of cross-linked poly(ethylene glycol diacrylate) (XLPEGDA) and XLPEGDA/TiO_2 membranes with a focus on CO_2", *Energy Fuel*, **32**, 5418 (2018).
11. H. Q. Lin and B. D. Freeman, "Gas permeation and diffusion in cross-linked poly(ethylene glycol diacrylate)", *Macromolecules*, **39**, 3568 (2005).
12. A. Sabetghadam, X. Liu, S. Gottmer, L. Chu, J. Gascon, and F. Kapteijn, "Thin mixed matrix and dual layer membranes containing metal-organic framework nanosheets and Polyactive™ for CO_2 capture", *J. Membr. Sci.*, **570-571**, 226 (2019).
13. J. E. Shin, S. K. Lee, Y. H. Cho, and H. B. Park, "Effect of PEG-MEA and graphene oxide additives on the performance of Pebax®1657 mixed matrix membranes for CO_2 separation", *J. Membr. Sci.*, **572**, 300 (2019).
14. S. Bandehali, A. Moghadassi, F. Parvizian, S. M. Hosseini, T. Matsuura, and E. Joudaki, "Advances in high carbon dioxide separation performance of poly (ethylene oxide)-based membranes", *J. Energy Chem.*, **46**, 30 (2020).
15. N. U. Kim, B. J. Park, M. D. Guiver, and J. H. Kim, "Use of non-selective, high-molecular-weight poly(ethylene oxide) membrane for CO_2 separation by incorporation of comb copolymer", *J. Membr. Sci.*, **605**, 118092 (2020).
16. J. Deng, Z. Dai, J. Yan, M. Sandru, E. Sandru, R. J. Spontak, and L. Deng, "Facile and solvent-free fabrication of PEG-based membranes with interpenetrating networks for CO_2 separation", *J. Membr. Sci.*, **570-571**, 455 (2019).
17. H. Lin and B. D. Freeman, "Gas solubility, diffusivity and permeability in poly(ethylene oxide)", *J. Membr. Sci.*, **239**, 105 (2004).
18. H. J. Min, M. Kang, C. S. Lee, and J. H. Kim, "Dual-functional interconnected pebble-like structures in highly crystalline poly (ethylene oxide) membranes for CO_2 separation", *Sep. Purif. Technol.*, **263**, 118363 (2021).
19. S. Feng, J. Ren, K. Hua, H. Li, X. Ren, and M. Deng, "Poly(amide-12-b-ethylene oxide)/polyethylene glycol blend membranes for carbon dioxide separation", *Sep. Purif. Technol.*, **116**, 25 (2013).
20. X. Mei Wu, Q. Gen Zhang, P. Ju Lin, Y. Qu, A. Mei Zhu, and Q. Lin Liu, "Towards enhanced CO_2 selectivity of the PIM-1 membrane by blending with polyethylene glycol", *J. Membr. Sci.*, **493**, 147 (2015).
21. I. Hossain, D. Kim, A. Z. Al Munsur, J. M. Roh, H. B. Park, and T.-H. Kim, "PEG/PPG−PDMS-based cross-linked copolymer membranes prepared by ROMP and in situ membrane casting for CO_2 separation: an approach to endow rubbery materials with properties of rigid polymers", *ACS Appl. Mater. Interfaces*, **12**, 27286 (2020).
22. I. Jeong, I. Hossain, A. Husna, and T.-H. Kim, "Development of CO_2-philic blended membranes using PIM−PI and PIM−PEG/PPG", *Macromol. Mater. Eng.*, **308**, 2200596 (2023).
23. T. Khosravi and M. Omidkhah, "Preparation of CO_2-philic polymeric membranes by blending poly(ether-b-amide-6) and PEG/PPG-containing copolymer", *RSC Advances*, **5**, 12849 (2015).
24. D. Kim, I. Hossain, Y. Kim, O. Choi and T.-H. Kim, "PEG/PPG-PDMS-adamantane-based cross-linked terpolymer using the ROMP technique to

prepare a highly permeable and CO_2-selective polymer membrane", *Polymers*, **12**, 1674 (2020).
25. S. Yu, S. J. An, K. J. Kim, J. H. Lee, and W. S. Chi, "High-loading poly(ethylene glycol)-blended poly(acrylic acid) membranes for CO_2 separation", *ACS Omega*., **8**, 2119 (2023).
26. X. Lu and R. A. Weiss, "Phase behavior of blends of poly(ethylene glycol) and partially neutralized poly(acrylic acid)", *Macromolecules*, **28**, 3022 (1995).
27. R. M. Lilleby Helberg, Z. Dai, L. Ansaloni, and L. Deng, "PVA/PVP blend polymer matrix for hosting carriers in facilitated transport membranes: Synergistic enhancement of CO_2 separation performance", *Green Energy Environ*., **5**, 59 (2020).
28. E. M. Abdelrazek, A. M. Abdelghany, S. I. Badr, and M. A. Morsi, "Structural, optical, morphological and thermal properties of PEO/PVP blend containing different concentrations of biosynthesized Au nanoparticles", *J. Mater. Res. Technol.*, **7**, 419 (2018).
29. N. S. Vrandečić, M. Erceg, M. Jakić, and I. Klarić, "Kinetic analysis of thermal degradation of poly(ethylene glycol) and poly(ethylene oxide)s of different molecular weight", *Thermochim. Acta*., **498**, 71 (2010).
30. C. Wang, T. Yang, W. Zhang, H. Huang, Y. Gan, Y. Xia, X. He, and J. Zhang, "Hydrogen bonding enhanced SiO_2/PEO composite electrolytes for solid-state lithium batteries", *J. Mater. Chem. A*., **10**, 3400 (2022).
31. N. Chen, X. Yao, C. Zheng, Y. Tang, M. Ren, Y. Ren, M. Guo, S. Zhang, and L.-Z. Liu, "Study on the miscibility, crystallization and crystalline morphology of polyamide-6/polyvinylidene fluoride blends", *Polymer*, **124**, 30 (2017).
32. A. K. Khasanova and B. A. Wolf, "PEO/$CHCl_3$. Crystallinity of the polymer and vapor pressure of the solvent. Equilibrium and nonequilibrium phenomena", *Macromolecules*, **36**, 6645 (2003).
33. B. Crist and J. M. Schultz, "Polymer spherulites: A critical review", *Prog. Polym. Sciv*, **56**, 1 (2016).
34. H.-L. Chen, L.-J. Li, and T.-L. Lin, "Formation of segregation morphology in crystalline/amorphous polymer blends: Molecular weight effect", *Macromolecules*, **31**, 2255 (1998).
35. M. Yang and C. Gogos, "Crystallization of poly(ethylene oxide) with acetaminophen − A study on solubility, spherulitic growth, and morphology", *Eur. J. Pharm. Biopharm.*, **85**, 889 (2013).
36. S. Bertoni, B. Albertini, and N. Passerini, "Spray congealing: An emerging technology to prepare solid dispersions with enhanced oral bioavailability of poorly water soluble drugs", *Molecules*, **24**, 3471 (2019).
37. J. Li, S. Wang, K. Nagai, T. Nakagawa, and A. W. H. Mau, "Effect of polyethyleneglycol (PEG) on gas permeabilities and permselectivities in its cellulose acetate (CA) blend membranes", *J. Membr. Sci.*, **138**, 143 (1998).
38. M. Kang, H. J. Min, N. U. Kim, and J. H. Kim, "Amphiphilic micelle-forming PDMS-PEGBEM comb copolymer self-assembly to tailor the interlamellar nanospaces of defective poly(ethylene oxide) membranes", *Sep. Purif. Technol.*, **257**, 117892 (2021).
39. J. H. Lee, J. Y. Lim, M. S. Park, and J. H. Kim, "Improvement in the CO_2 permeation properties of high-molecular-weight poly(ethylene oxide): use of amine-branched poly(amidoamine) dendrimer", *Macromolecules*, **51**, 8800 (2018).
40. Z.-X. Wang, W.-H. Zhang, G. Yu, M.-J. Yin, S. Li, and Q.-F. An, "Defect-free PEO membrane fabrication by hydrogen bonding coupling thermal annealing for carbon capture", *Chem. Eng. Sci.*, **282**, 119354 (2023).
41. K. W. Yoon and S. W. Kang, "Highly permeable and selective CO_2 separation membrane to utilize 5-hydroxyisophthalic acid in poly(ethylene oxide) matrix", *Chem. Eng. J.*, **334**, 1749 (2018).